Current Biology 23, 1649–1657, September 9, 2013 ©2013 Elsevier Ltd All rights reserved http://dx.doi.org/10.1016/j.cub.2013.07.028

Article

The *Dionaea muscipula* Ammonium Channel *DmAMT1* Provides NH_4^+ Uptake Associated with Venus Flytrap's Prey Digestion

Sönke Scherzer,[1,5] Elzbieta Krol,[1,2] Ines Kreuzer,[1] Jörg Kruse,[3] Franziska Karl,[1] Martin von Rüden,[1] Maria Escalante-Perez,[1] Thomas Müller,[1] Heinz Rennenberg,[3] Khaled A.S. Al-Rasheid,[4] Erwin Neher,[5,*] and Rainer Hedrich[1]

[1]Institute for Molecular Plant Physiology and Biophysics, Julius-von-Sachs Platz 2, 97082 Würzburg, Germany

[2]Department of Biophysics, Maria Curie-Skłodowska University, 20-033 Lublin, Poland

[3]Institute of Forest Sciences, University of Freiburg, Georges-Koehler-Allee 53/54, 79085 Freiburg, Germany

[4]Zoology Department, College of Science, King Saud University, P.O. Box 2455, Riyadh 11451, Saudi Arabia

[5]Department for Membrane Biophysics, Max Planck Institute for Biophysical Chemistry, 37077 Goettingen, Germany

Summary

Background: Ammonium transporter (AMT/MEP/Rh) superfamily members mediate ammonium uptake and retrieval. This pivotal transport system is conserved among all living organisms. For plants, nitrogen represents a macronutrient available in the soil as ammonium, nitrate, and organic nitrogen compounds. Plants living on extremely nutrient-poor soils have developed a number of adaptation mechanisms, including a carnivorous lifestyle. This study addresses the molecular nature, function, and regulation of prey-derived ammonium uptake in the Venus flytrap, *Dionaea muscipula*, one of the fastest active carnivores.

Results: The *Dionaea muscipula* ammonium transporter DmAMT1 was localized in gland complexes where its expression was upregulated upon secretion. These clusters of cells decorating the inner trap surface are engaged in (1) secretion of an acidic digestive enzyme cocktail and (2) uptake of prey-derived nutrients. Voltage clamp of *Xenopus* oocytes expressing DmAMT1 and membrane potential recordings with DmAMT1-expressing *Dionaea* glands were used to monitor and compare electrophysiological properties of DmAMT1 in vitro and in planta. DmAMT1 exhibited the hallmark biophysical properties of a NH_4^+-selective channel. At depolarized membrane potentials (V_m = 0), the K_m (3.2 ± 0.3 mM) indicated a low affinity of DmAMT1 for ammonium that increased systematically with negative going voltages. Upon hyperpolarization to, e.g., −200 mV, a K_m of 0.14 ± 0.015 mM documents the voltage-dependent shift of DmAMT1 into a NH_4^+ transport system of high affinity.

Conclusions: We suggest that regulation of glandular DmAMT1 and membrane potential readjustments of the endocrine cells provide for effective adaptation to varying, prey-derived ammonium sources.

Introduction

Ammonium (NH_4^+) transport is a key process in nitrogen metabolism, and ammonium transporters form a conserved family of proteins widely distributed over all domains of life. Among the species studied, ammonium transporters (AMTs) have been identified and functionally analyzed from man to microbe. Members of the human ammonium transporters Rhesus factor AMT/Rh family play a critical role in renal NH_4^+ excretion and collecting duct ammonium transport [1]. In contrast, some chemoautotrophic bacteria are able to gain energy via ammonia oxidation. The genome of *Nitrosomonas europaea* as bacterial example contains a single gene (*Rh1*) that belongs to the AMT/Rh ammonium transporter family. When expressed in yeast (*Saccharomyces cerevisiae*) ammonium-transport-deficient mutants, the function of Rh1 as an ammonia (NH_3) transporter was suggested [2]. Ammonium transporters of *Saccharomyces cerevisiae* itself were found to be essential for fast growth at very low ammonia concentrations [3]. Within green algae such as *Chlamydomonas reinhardtii* and salt-resistant *Dunaliella viridis*, ammonium transporters represent important elements of the nitrogen nutrition system [4, 5].

In many higher plants, ammonium is the preferred nitrogen source [6]. For its uptake, the genome of higher plants contains two families of ammonium transporters, AMT1 and AMT2 [7–9]. Both families show a high affinity for ammonium, and transport saturates rapidly at low millimolar concentrations [7, 10–16]. But, contrary to AMT1 transporters, those belonging to the AMT2 family are unable to transport the ammonium analog methylammonium ($CH_3NH_3^+$) and possess a smaller transport capacity [8, 17].

Plant AMT1 transporters can apparently be divided into two subbranches [18]. One population is not affected by changes in the external proton concentration [13, 16, 19, 20], and another is more active in acidic extracellular environments [9, 11, 14]. AMTs have thus been predicted to serve either as NH_4^+ channels or as proton-coupled NH_3 transporters. Upon mutagenesis, the two major transport modes even seem to interconvert [9, 11, 14]. Ammonium as a cation can be taken up following the electrical gradient. Hence, upon addition of NH_4^+ the cell membrane will depolarize.

Ammonium transport was analyzed in planta via $^{13}NH_4^+$ flux analyses [21] and by electrophysiological approaches. Inward movement of positive charge carried by NH_4^+ ions causes a drop in membrane potential [10]. In nutrient solution containing no nitrogen, the membrane potential of plant underground cell types such as the rice root was −131 mV. Introduction of 100 μM NH_4^+ to the bathing medium causes rapid depolarization to −89 mV [22].

So far, ammonium currents causing membrane depolarization have not been measured in plant cells. Direct measurements of currents resulting from transmembrane NH_4^+ fluxes, however, were accomplished by transfer of "green" AMT genes into expression systems, which are free of any plant ammonium transporter, such as *Xenopus laevis* oocytes. Using this system, with proper voltage clamp conditions allowed, AMT-mediated ammonium currents in the low submicroampere range were recorded [9, 13, 16, 19, 20, 23, 24]. Under double-electrode voltage clamp (DEVC) conditions, these NH_4^+ stimulated inward currents with, e.g., PvAMT1;1 from common bean increased when the external pH was decreased from 7.0

*Correspondence: eneher@gwdg.de

to 5.5 [11]. In contrast, NH_4^+ currents with AtAMT1;1 from the model plant *Arabidopsis thaliana* were not found to be sensitive to extracellular pH changes [13]. This would assign PvAMT1;1 a H^+-coupled NH_4^+ transport mechanism and AtAMT1;1 a channel-like behavior.

AMTs are not restricted to roots but were also localized in above-ground plant tissue. In photosynthetic cells, for example, AMTs seem to be important for retrieval of NH_4^+ liberated during photorespiration [8, 12, 15, 23]. Carnivorous plants adapted to nutrient-poor soils catch small animals to meet their macro- and micronutrient demand. When visiting the bilobed leaf structures of *Dionaea muscipula* traps, prey comes into contact with the touch sensors of the trap, triggering its closure within a fraction of a second. Each contact triggers an action potential (AP), and two subsequent APs activate the motor center to release the viscoelastic energy, which closes the snap trap. Attempting to escape, the entrapped animal consecutively touches the sensory organs and triggers synthesis of a touch hormone. As a result, the trap lobes seal hermetically to form a "green stomach." With insect prey, densely packed gland complexes at the inner surface secrete an acidic hydrolase cocktail containing chitinases, proteases, nucleases, lipases, and phosphatases [25, 26].

In this study on the Venus flytrap, we analyzed (1) ammonium production by the acid protease mixture of the "green stomach," (2) NH_4^+ uptake into the glands, and (3) the nature and characteristics of DmAMT1, the ammonium transporter involved. We showed that *Dionaea muscipula* induces expression of an electrogenic AMT moiety upon secretion and that DmAMT1 is localized in the glands that take up prey-derived NH_4^+.

Results

Prey Digestion Associated with Ammonium Production

Our previous studies have shown that Venus flytrap in the process of prey capture produces the oxilipine-type touch hormone 12-oxo-phytodienoic acid (OPDA) [25]. When OPDA derivatives in general and the hyperactive molecular mimic coronatine (COR) in particular are applied, glands present at the inner surface of *Dionaea*'s trap lobes secrete an acidic as well as lytic enzyme cocktail. This exocytotic protein moiety contains more than 20 different hydrolases, including a set of diverse proteases. Thus, the question arises, what are the major products of prey digestion? When 5, 10, and 20 mg insect powder were incubated for 15 hr with 200 μl flytrap digestive fluid collected from COR-treated traps (pH 4.3), a parallel increase in NH_4^+ was observed (Figure S1A available online). To get deeper insights in this issue, we incubated casein, a well-defined animal protein with secreted fluid. Digestion of casein also resulted in a linear increase of ammonium concentration (Figure S1A) and in production of a complex set of amino acids, which were not present in the secreted fluid. We found every component of the digested casein protein, but glutamine (GLN) was underrepresented (Figure S1B). While casein consists of 8.8% glutamine, after digestion only 0.3% ± 0.004% was detected. The fact that glutamine but not asparagine (ASN) (3.6% before and 3.8% ± 0.18% after digestion) was of low abundance in the casein-derived samples points to a glutamine deaminase activity associated with the *Dionaea*-secreted fluid. This enzymatic deaminase activity was corroborated by digestion of just glutamine in the secreted fluid, which also produced ammonium. In contrast, heat-inactivated enzyme containing fluid was not able to digest glutamine or to produce ammonium (Figure S1C). This indicates that inside the hermetically sealed acidic "green stomach" glutamine deamination and hydrolysis of natural N-rich components derived from prey give rise to NH_4^+ production.

Digestion-Activated Glands Become Ammonium Uptake Competent

To address the question of whether the Venus flytrap takes up the digestion-derived ammonium, we fed plants with insect powder dissolved in a solution containing 1 mM $^{15}NH_4^+$ (99 atom% ^{15}N). We observed immediate uptake of ^{15}N during the first hours after incubation onset, averaging 2.67 ± 0.48 $\mu mol\ g^{-1}\ h^{-1}$ (Figure 1A). To further investigate the NH_4^+ uptake capability of *Dionaea*'s glands, we used an electrophysiological approach. Therefore, single lobes of open traps and those of "stomach"-forming, digesting ones were fitted on a support. Glands of each lobe were initially monitored by current-clamp microelectrodes for excitability of the endocrine cells. Bending of the sensory hairs depolarized the membrane from its resting state to values more positive than −60 mV, eliciting APs, which spread over the whole trap (Figure S1D). Two APs within a short time lead to trap closure (Figure S1E), a phenomenon well known for this excitable, carnivorous plant [27]. Upon impalement of nonstimulated single gland cells with voltage-recording electrodes, resting potentials around −116 mV were recorded (Figure 1B, black line). With nonsecreting glands, the exposure to 100 μM NH_4^+ almost did not affect the resting state of the endocrine cells. Increase of the ammonium level 10- or even 100-fold depolarized the cells only weakly (20 mV). This situation changed fundamentally when glands were taken from traps in the process of digesting a prey that had been captured 1–2 days before or when secretion was induced by COR stimulation for 12 hr [25]. Challenge of such cells in the secreting state with pH 6 buffered perfusion with 0.1, 1, and 10 mM NH_4^+ solutions resulted in a progressive depolarization (Figure 1B, red line). Compared to cells in the nonsecreting state, the prestimulus potential was about −145 mV, and was thus 20 mV more hyperpolarized. With COR-activated gland cells, application of 0.1 mM NH_4^+ was already followed by a 20 mV depolarization. Upon steps to 1 mM concentrations of the trigger cation, the membrane potential dropped to below −80 mV, while upshifts to 10 mM resulted in peak depolarization amplitudes of 100 mV or more. Such peak NH_4^+ depolarizations to potentials positive to −60 mV triggered action potentials of the same endpoint depolarization as the mechanical-induced test AP at the beginning of the experiment, which under the given experimental surroundings was about 0 mV. After removal of the given NH_4^+ stimulus, the resting state of secreting gland cells of −140 mV was reached again (Figure 1B). Similar experiments were performed with a series of six different extracellular NH_4^+ levels, and depolarization amplitudes were plotted as a function of the ammonium dose. Figure 1C depicts such NH_4^+ saturation curves for stimulated and nonstimulated gland cells. Fitting the data with the Michaelis-Menten equation allowed us to calculate an apparent K_m value of 0.47 and 1.34 mM for secreting and nonsecreting endocrine cells, respectively. These results indicate that, in contrast to open trap lobes, gland cells of the digesting *Dionaea* stomach operate an electrogenic, high-affinity NH_4^+ uptake system.

In order to determine whether this transport system is energized by the transmembrane proton gradient, we varied the

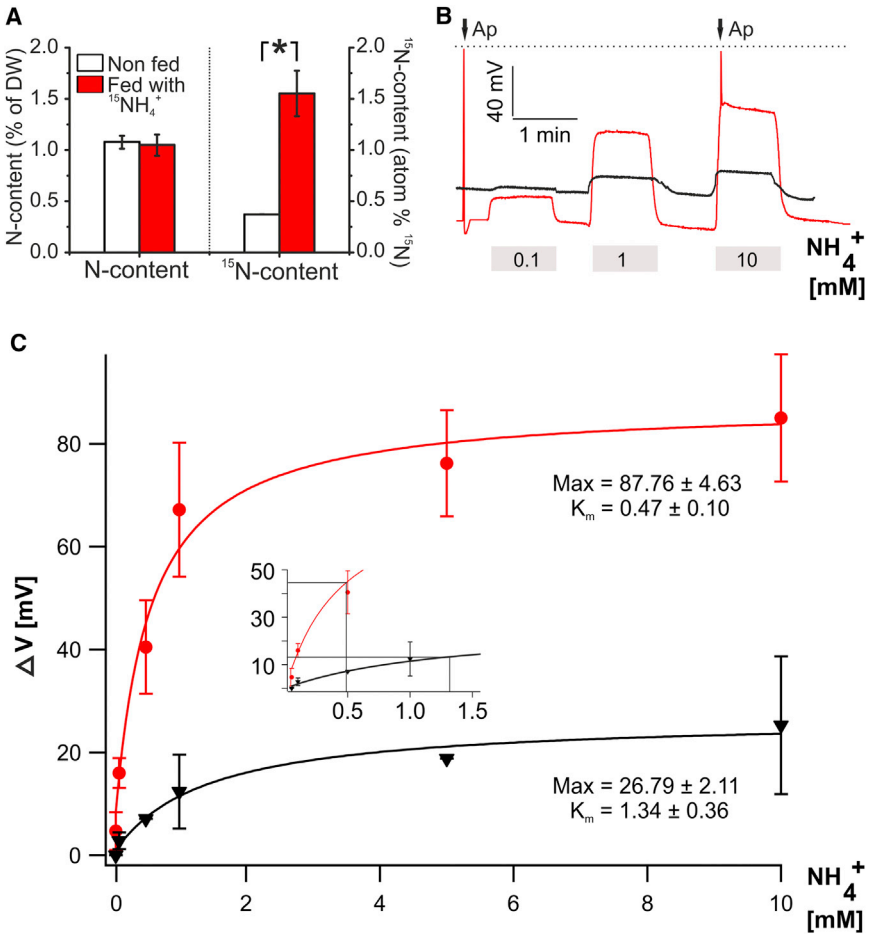

Figure 1. Uptake of NH_4^+ by Glands of *Dionaea muscipula*

(A) Plants were fed with 20 mg insect powder that was dissolved in 100 μl solution containing 1mM $^{15}NH_4^+$ (99 atom% ^{15}N). Incubation was stopped after 3 hr; traps were thoroughly rinsed with distilled water, dried for 2 days at 65°C, and subsequently pulverized with a ball mill. Between 1 and 2 mg dried material was weighed into tin capsules for total nitrogen and ^{15}N determination using an elemental analyzer coupled to an IRMS. Rates of NH_4^+ uptake amounted to 2.67 ± 0.48 μmol g^{-1} h^{-1}. Asterisks indicate statistically significant difference ($p < 0.01$ by one-way ANOVA; $n \geq 4$, mean ± SD).

(B) Membrane voltage responses of *Dionaea muscipula* gland cells to different NH_4Cl concentrations (as indicated). Glands stimulated for digestion revealed a resting potential of −145.1 ± 16.4 mV (n = 9, mean ± SD; red line). Just before NH_4Cl was addressed, intracellular localization of the measuring electrode was confirmed by touching trigger hair and hence evoking mechanical AP; note that such an AP did also appear when 10 mM NH_4Cl was applied. The membrane potential of unstimulated gland cells (black line) exhibited higher resting potential (−115.8 ± 15.2 mV [n = 13, mean ± SD]) and smaller NH_4Cl-induced depolarization. The dotted line represents 0 mV.

(C) Dose response curves of nondigesting (black line) or digesting (red line) glands; with the fit to Michaelis-Menten equation $[f(x) = (\Delta V_{max} \cdot x) / (K_m + x)]$. K_m values were calculated as follows: digesting glands = 471.94 ± 103 μM; nondigesting glands = 1336 ± 359 μM. Inset between the fits presents magnification with indicated K_m concentrations.

See also Figure S1.

external proton concentration over a broad range. These experiments revealed that the external pH itself has only little impact on resting membrane potential, indicating weak proton conductance of gland cell plasma membrane (Figure S4B). Addition of ammonium to stimulated and nonstimulated traps documented that the flytraps gland NH_4^+ transporter is not affected by even up to 10.000-fold changes in proton-motive force (Figure S4C). This COR-inducible *Dionaea* ammonium transporter was thus classified as pH independent and of moderate high affinity for its cationic substrate NH_4^+.

Activated *Dionaea* Glands Express DmAMT1

To identify the gene encoding the gland ammonium transporter characterized in intact traps, we searched a *Dionaea muscipula* expressed sequence tag (EST) collection (generated just recently by Schulze et al. [26]) with nucleotide sequences of ammonium transporters previously identified in plants. Thereby, we identified a transcript homologous to type I ammonium transporters (Figure S2A; see [28] for a review). We were able to amplify and clone the full-length sequence, which we termed DmAMT1 in analogy to the first ammonium transporter identified in *Arabidopsis thaliana* AtAMT1;1. Based on an alignment with selected protein sequences of mammalian, plant, bacterial, and fungal ammonium transporters of the AMT/MEP/Rh family, we generated a phylogenetic tree (Figure S2B). Within this tree, DmAMT1 appeared to close the gap between plants and other members of this family in different other kingdoms. In *Arabidopsis*, six genes encoding AMTs have been identified and characterized so far [8, 15, 21]. While most of them are thought to be involved in ammonium uptake from the soil, DmAMT1 showed quite high transcript levels in traps and especially in gland tissue (Figures 2A and S2). On the other hand, DmAMT1 expression was rather low in gland-free green organs such as petioles and flowers. We therefore assume that DmAMT1 is required for the uptake of prey-derived NH_4^+ via the glands of the "green stomach." Interestingly, DmAMT1 expression could be further enhanced by COR stimulation. Coronatine binds the COI1 jasmonate receptor [29], which in *Dionaea* is inducing pronounced and prolonged secretion [25]. In secreting traps and especially in gland cells—responsible for the release of digestive fluid but also for prey-derived nutrient uptake—DmAMT1 expression was induced nearly 4-fold (Figure 2B). Based on its gland- and secretion-related expression, we assume that DmAMT1 participates in the uptake of ammonium that is released from the digested prey.

DmAMT1 Carries Hallmark Characteristics of Gland Cell Ammonium Transporters

To compare the properties of DmAMT1 with the native NH_4^+-transport activity in gland cells, we injected DmAMT1 complementary RNA (cRNA) into *Xenopus* oocytes. In current-clamp measurements with the heterologous expression, system we could record NH_4^+-dependent changes in membrane

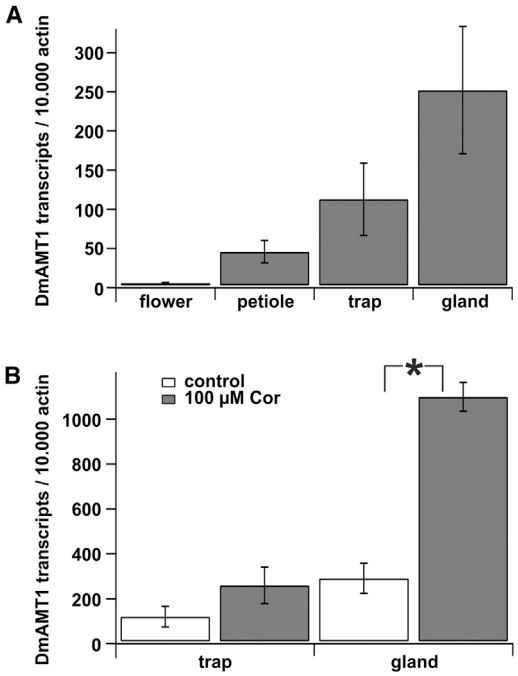

Figure 2. Expression Pattern of DmAMT1

(A) Quantification of DmAMT1 transcript levels in different aerial tissues. DmAMT1 transcripts were normalized to 10,000 molecules of DmACT (n = 3, mean ± SE).

(B) DmAMT1 expression was upregulated in traps and was even more pronounced in isolated glands 24 hr after application of 100 µM coronatine. Asterisks indicates statistically significant upregulation in gland tissue ($p < 0.01$ by one-way ANOVA; n = 3, mean ± SE).

See also Figure S2.

potential. While water-injected oocytes did not respond to challenges with 10 mM ammonium, DmAMT1-expressing ones depolarized by about 40 mV upon this kind of NH_4^+ stimulation (Figure 3A). During withdrawal of NH_4^+, the membrane potential repolarized to the prestimulus level. To resolve ionic currents underlying the depolarization associated with ammonium influx, we exposed DmAMT1-expressing oocytes in the voltage-clamp mode to chloride-based salts with a variety of monovalent cations. When in the bath solution 10 mM K^+ was replaced by 10 mM NH_4^+, pronounced inward currents were elicited (Figure 3B). These ammonium currents were only detectable in DmAMT1-expressing oocytes (Figures S3A–S3D). Similar results were obtained with shifts from Li^+-, Na^+-, K^+-, Rb^+-, Cs^+-, and $NMDG^+$-based chloride salts to NH_4Cl, indicating that DmAMT1 is NH_4^+ selective. Besides ammonium, a significant but less-pronounced $CH_3NH_3^+$ influx could be documented as well, amounting to 41.9% of that carried by NH_4^+ (Figure 3D). To further characterize selectivity, we investigated the membrane potentials of DmAMT1-expressing oocytes under different monovalent cation conditions (Figure 3C). Relative to $NMDG^+$, most of the tested ions evoked only small shifts in potential, indicating low permeability. Besides NH_4^+, only $CH_3NH_3^+$ specifically depolarized the cells showing a clear conductance of DmAMT1.

The *Escherichia coli* genome encodes a single ammonium transporter called AmtB. The atomic structure of AmtB, the first member of the Amt/MEP/Rh family to be characterized by crystallography, shows that these transporters form trimers. Each monomer supports a hydrophobic channel that appeared to conduct NH_3 rather than NH_4^+ ions [30, 31]. In contrast, earlier reports demonstrated voltage-dependent uptake currents in plant and microbial AMTs [13, 16, 19, 20]. In agreement with these results, our findings on DmAMT1 support the view of an electrogenic NH_4^+ transport. The DmAMT1 ammonium transporter homolog AMT1;1 from *Arabidopsis thaliana* requires distinct interactions between the trimer subunits for proper function [32]. A cytosolic C-terminal transactivation domain mediates this kind of allosteric regulation. Mutation of a conserved threonine T460 at a critical position of AtAMT1;1-4 in the hinge region of the C terminus leads to inactivation of the ammonium transporter [24, 33]. Since DmAMT1 and AtAMT1;1 share a homologous primary structure, we tested whether this threonine at position T464 in the *Dionaea* ammonium transporter is of crucial function as well. Replacement of threonine by alanine (T464A) or aspartate (T464D) rendered DmAMT1 NH_4^+ transport inactive (Figure S4A), indicating that C-terminal interaction between functional trimer subunits with the *Dionaea* class I plant AMT too is modulating the conductivity of the pore.

To compare the ammonium affinity of DmAMT1-expressing oocytes with that found in *Dionaea* glands, we clamped the plasma membrane of the frog cells at −140 mV, the resting potential of stimulated, secreting gland cells (c.f. Figure 1B) and increased the external NH_4^+ concentration in a stepwise manner. Similar studies were performed at −70 mV, representing a depolarized gland cell. At a holding potential of −70 mV, inward currents were observed already in response to bath NH_4^+ solutions containing levels as little as 30 µM of the cation (Figure S3E). Increase of the NH_4^+ dose further enlarged the amplitude of the inward current. Plotting the inward current as a function of the external ammonium level, we could fit a Michaelis-Menten equation, revealing a $K_{m\ -70\ mV}$ of 0.82 ± 0.04 mM (Figure 4B). In similar experiments, clamping of the oocyte at the resting potential of activated gland cells, dose-response-curve analysis revealed a $K_{m\ -140\ mV}$ of 0.26 ± 0.007 mM (Figure 4A). Through comparison of the ammonium uptake in DmAMT1-expressing oocytes (red line) with the dose-response curves from digesting *Dionaea* glands (black line), strong similarities could be observed with K_m values in the same range (Figure 4A). The oocyte experiments show that the affinity of DmAMT1 to its cationic substrate is voltage dependent. To study this matter in more detail, we extended the K_m/V analysis to a voltage window from −200 to 0 mV, covering the physiological membrane potential range of *Dionaea*. This K_m/V analysis, depicted in Figure 4B, supports the notion that the ammonium transporter affinity is a function of voltage. Plant ammonium transporters have been categorized by their apparent substrate dependency into high- and low-affinity types. The generally accepted threshold between high- and low-affinity AMTs is 1 mM [7, 12, 22, 34]. For this classification to be applied to our measurements, the membrane potential has to be considered. In the absence of an electrical driving force (0 mV and oocyte intracellular NH_4^+ level being rather low), ammonium was just driven by its concentration gradient. For half-maximal transport activity, 3.2 ± 0.28 mM cation was required at this potential (Figure 4B). When in addition to the chemical gradient of NH_4^+ an electrical gradient was applied, the K_m dropped to values in the submillimolar range. Upon hyperpolarization to −180 mV, DmAMT1 was operating on the basis of a K_m of 0.17 ± 0.02 mM. Thus, in the physiological membrane potential range of *Dionaea* in general and that of activated

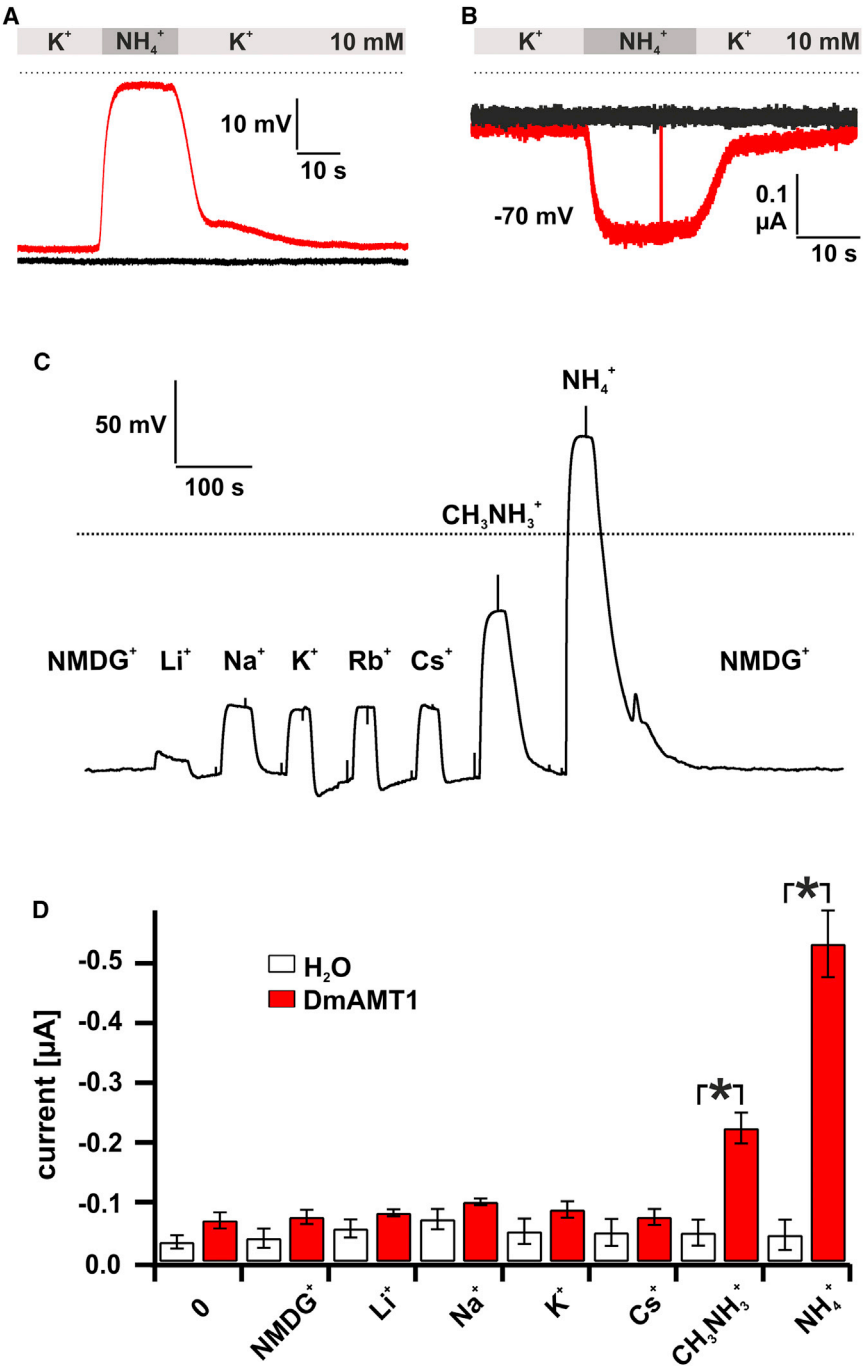

Figure 3. Selectivity of DmAMT1 Expressed in *Xenopus* Oocytes

(A and B) Membrane voltage depolarization (A) and current changes (B) recorded in DmAMT1-expressing *Xenopus* oocytes (red lines) in response to NH_4Cl (as indicated). Control water-injected oocytes did not show any ammonium sensitivity (black lines). The dotted line represents 0 mV/µA.

(C) Reversal potentials of DmAMT1-expressing oocytes for different monovalent cations in the bath solution over time. Between testions, oocytes were perfused with $NMDG^+$. Differences of potentials against $NMDG^+$ (ΔVrev x = Vrev x − Vrev $NMDG^+$; ΔVrev Li^+ = 10.75 ± 5.56 mV, ΔVrev Na^+ = 30.5 ± 7.32 mV, ΔVrev K^+ = 32.67 ± 2.31 mV, ΔVrev Rb^+ = 31.33 ± 5.68 mV, ΔVrev Cs^+ = 31.67 ± 3.51 mV, ΔVrev $CH_3NH_3^+$ = 70 ± 20.7 mV, and ΔVrev NH_4^+ = 169 ± 21.79 mV) indicate specific conductance for $CH_3NH_3^+$ and NH_4^+. The dotted line represents 0 mV. Standard bath solution contained 10 mM of the respective cation, and osmolarity was adjusted to 220 mosmol/kg with D-sorbitol (n = 4, mean ± SD).

(D) Currents recorded at −200 mV of oocytes injected with H_2O (empty bars) or DmAMT1 cRNA (filled bars) in the presence of different cation containing bath solutions. Asterisks indicate statistically significant different currents in $CH_3NH_3^+$ and NH_4^+ ($p < 0.01$ by one-way ANOVA; n = 5, mean ± SD).

See also Figure S3.

gland cells in particular, DmAMT1 mediates high-affinity NH_4^+ transport (Figure 4B).

Assuming (1) a single binding site for ammonium, as indicated by the Michaelis-Menten kinetics, and (2) a ammonium concentration at this point that is in electrochemical equilibrium with the bath medium, we calculated the binding site location as it was first described for blockage of sodium channels [35]. Using this procedure, we located the ammonium binding site of DmAMT1 at (δ = 0.409 ± 0.007) 41% within the membrane electrical field (Figure 4B). To test whether the proton-motive force drives this gland cell ammonium transporter, in addition to the electrochemical potential, we varied the pH between 8 and 4. Changes in the external proton concentration of up to 10.000-fold, however, affected neither the activity nor the voltage dependence of DmAMT1 expressed in *Xenopus* oocytes (Figure S6D). These results are reinforced by the pH independence of ammonium-induced depolarization in *Dionaea* gland cells (Figure S6C). While ammonium transporters studied in *Xenopus* oocyte expression system generally mediate inward NH_4^+ currents in the submicroampere range [9, 19, 20, 23, 24], with DmAMT1, currents of up to 4 µA could be recorded (Figures S3D and S4E). This fact and a near-Nernstian response in membrane potential upon a 10-fold change in bath NH_4^+ concentration (Figure 4C) suggested that DmAMT1 might operate in the ion channel mode (see [36] for a review on ion channels in plants). Nernstian-type ion channel transport can be distinguished from a carrier-mediated one on the basis of their activation energy Q_{10}. To obtain the Q_{10} of DmAMT1 with oocytes exhibiting the *Dionaea* ammonium transport activity, we determined the temperature dependence between 10°C and 30°C of the NH_4^+ current amplitude. Change of the temperature profile affected the DmAMT1-dependent NH_4^+ currents only weakly (Figures S4F and S4G), and the Q_{10} value of 1.26 ± 0.09 derived from Arrhenius plotting classifies the gland cell ammonium transport activity as channel like [24, 34].

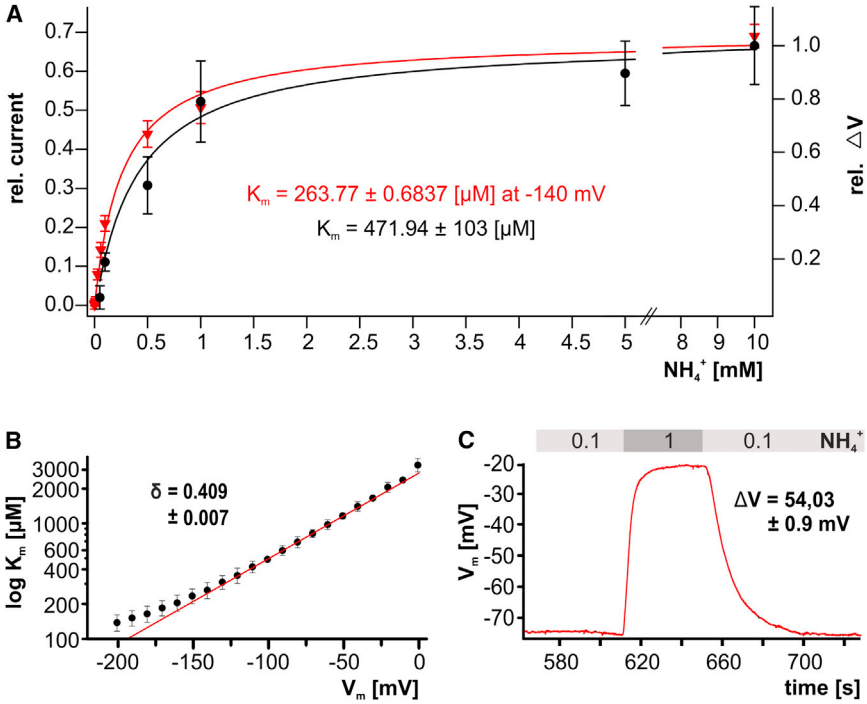

Figure 4. Electrophysiological Characterization and Nernst Behavior of DmAMT1

(A) Michaelis-Menten fit of a dose-response curve of DmAMT1 expressed in *Xenopus* oocytes at −140 mV voltage clamp (red line), and membrane depolarization by NH_4^+ uptake in digesting glands (black line) with respective K_m values. Different NH_4Cl concentrations were complemented with KCl for proper osmolar/cation adjustment (n = 5, mean ± SD).

(B) K_m dependency on clamped voltage. Data were fitted with an exponential function [$K_m = K_{m0} \exp(\delta z F V_m / R T)$]. Since zF/RT = 0.0417 mV^{-1}, the resulting parameters were $K_{m\,0}$ = 2732.77 ± 74.8 μM and δ = 0.409 ± 0.007 (n = 5). The fact that measured K_m values at potentials negative from −150 mV appear higher than estimated by the fit is due to diffusion limitations. With high transport rates at hyperpolarized membrane potentials, the ammonium concentration at its specific binding site inside the pore is lower compared to the bath concentration. Currents and voltages were recorded with standard bath solution containing indicated NH_4Cl concentrations.

(C) Membrane potential of a DmAMT1-expressing oocyte in response to 0.1 and 1 mM NH_4Cl. Change of the ammonium concentration by a factor of ten leads to a mean shift in membrane potential of 54.03 ± 0.9 mV (n = 4, mean ± SD). Currents were recorded with standard bath solution containing indicated NH_4Cl concentrations. See also Figure S4.

Discussion

Dionaea Endocrinology

Carnivorous plants such as *Dionaea muscipula* are living on nitrogen-depleted soils and overcome nutrient limitations of their environment by catching and digesting nitrogen-rich animals. Early on, it was recognized that the trap lobes of the excitable plant *Dionaea muscipula* possess numerous digestive glands that comprise two apical layers of head cells responsible for secretion and nutrient uptake, followed by basal endodermoid cells that mediate exchange with the surrounding tissue [37, 38]. These glands do not secrete until stimulated by natural or artificial prey [27, 39]. This demonstrated that secretion depends upon exposure to elicitors and takes place during the predatory phase. This stage is also concomitant with expression of hydrolase- and demand-dependent nutrient transporter genes [37, 40]. With *Dionaea* glands, a wide range of low-molecular-weight nitrogen compounds was found to cause the secretion of both Cl^- and acid proteolytic activity [38, 41]. Unlike the human endocrine system, glands in the "green stomach" of the *Dionaea* trap sense the chemistry of the prey, secrete a decomposing enzyme cocktail, and take up nitrogen-rich components. Thus, the flytrap operates like a mouth-stomach-intestine unit. The ammonium transporter DmAMT1 might well represent one of the dominant transporters required for the uptake of nitrogen in this fascinating organ.

Transcriptional Regulation of Plant AMTs

In noncarnivorous plants growing on a nitrogen-rich support, ammonium is taken up via the roots. A series of studies correlating transcripts or protein levels with ammonium influx or employing promoter-reporter gene analyses indicated that transcriptional control in response to the nutritional status is a major regulatory mechanism for the activity of AMTs in plants ([15]; see [18] for s review). In tomato roots, e.g., NH_4^+ produced by N_2-fixing bacteria is able to induce the expression of the respective ammonium transporter gene LeAMT1;2 [42].

The ammonium transporter DmAMT1, which we identified in the flytrap, is expressed in glands covering the surface of the "green stomach," and DmAMT1 transcription is associated with the prey recognition-digestion cycle. Prey-dependent DmAMT1 transcription could be mimicked by stimulation of *Dionaea* traps with the touch hormone mimicry COR, which initiates secretion [25]. With application of COR, a rise in DmAMT1 messenger RNA (mRNA) in gland cells was already observed 4 hr after stimulus onset (Figure S2C). In contrast to the situation known from most root-localized ammonium transporters in other noncarnivorous plants (see above), DmAMT1 is not transcriptionally induced by its substrate (Figure S2D). While the latter is generated during ongoing prey protein decomposition by the secreted fluid, DmAMT1 expression is immediately triggered at secretion onset after prey capture or COR treatment. This is well in line with our finding that glands of the Venus flytrap do not depolarize notably in response to NH_4^+ exposure until secretion is induced (Figures 1B and 1C), a finding in agreement with Darwin's 1875 observation concerning secretion elicitors [27].

Interestingly, the ammonium transporter NaAMT1 in the pitcher plant *Nepenthes alata* has a similar localization (head cells of digestive glands in the lower part of the pitcher) and is induced after prey capture as well [43]. It is thus tempting to speculate that flesh-eating plants have not only adapted localization of their ammonium transporters but also their transcriptional regulation to suit the needs of their carnivorous life style.

While the transporter itself is not regulated by its substrate NH_4^+, stimulation of trap acidification was shown by Phil Rea

[39] to strongly depend on prey or elicitor preincubation. This fact together with the prey/COR induction of DmAMT1 suggests that uptake of prey-derived NH_4^+ might induce H^+ release, probably to keep the gland cell plasma membrane hyperpolarized [41]. The drop in pH to 3 or below activates a set of different hydrolases that digest the prey proteins. Among them—with ongoing protein degradation—a glutaminase would be able to generate a new GLN-derived NH_4^+ pool in addition to ammonium provided by the insect haemolymph [44]. This enzymatic activity might also be postulated from the fact that the rate of glutamine degradation (96.6%) observed in the secreted fluid exceeds by far the rate of chemical deamination (instability) of glutamine. Even at pH 2, glutamine levels would not decrease by more than 30% over a period of 2 weeks [45].

DmAMT1 NH_4^+ Channel Function and Voltage Regulation

Among the scientific community interested in ammonium transporters (AMT/MEP/Rh), a controversy exists regarding the actual transport mechanism represented by these proteins. Crystal-structure analysis and electrophysiological studies lead to contrary results concerning the modus operandi (channel or transporter), as well as the chemical form that is transported (NH_4^+ or NH_3) [16, 20, 30, 31].

Our finding of a weak temperature dependence of the Venus flytrap ammonium transporter DmAMT1 is consistent with a diffusion-controlled transport process. Similar results were reported for AtAMT1;2 [24]. Thus, the low activation energy together with Nernst dependence of NH_4^+ transport (Figures S4F, S4G, and 4C) indicate that the flytrap ammonium conductance in the glands could operate as an ion channel. In line with a channel-type mechanism, NH_4^+ currents associated with DmAMT1 were found not to depend on the external pH (Figures S4C and S4D). This result supports NH_4^+ as the transported species and renders NH_3 in symport with H^+ implausible. Moreover, with an equilibrium constant of $pK_a = 9.24$, the charged NH_4^+ ion is more abundant by orders of magnitude than the uncharged NH_3 at extracellular pH in plants and even more so at the extreme acidic conditions during prey digestion within the green stomach of the Venus flytrap. Increasing the electrical driving force for the cationic charge carrier, the NH_4^+ transport increased in near-ohmic/Goldman-like manner. Describing the dose-response curve with Michaelis-Menten kinetics (Figure 4A), one could estimate a K_m value, under the assumption that the permeating cation binds en passant to a single binding site. Furthermore, binding to this site is assumed to be at equilibrium with the outside medium. Such analysis at different membrane potentials demonstrates an increasing substrate affinity for NH_4^+ under hyperpolarized conditions. The dependence of K_m on voltage could be well fitted by an exponential function over a 100 mV voltage range (Figure 4B). This voltage-dependent K_m, together with the electrogenic transport, indicates that the molecular species most likely transported by DmAMT1 is NH_4^+ and not the uncharged NH_3. The interaction between the positively charged substrate and its channel increases with negative going membrane potentials, leading to an increased affinity (cf. [9, 11, 16, 19]).

Conclusions

In this study on the Venus flytrap, we analyzed the molecular mechanisms of production and uptake of prey-derived nitrogen compounds. Upon recognition of prey and its capture, a hermetically sealed acidic "green stomach" is formed and protein-rich tissue is broken down into peptides and amino acids. Deamination of glutamine produces NH_4^+. Ammonium ions represent the substrates of DmAMT1, channeling nitrogen-based cations into the gland cells. The biophysical properties of DmAMT1 and its transcriptional activation in secreting gland cells are well suited to fit ammonium acquisition of the "green stomach." Regulation of DmAMT1 density and NH_4^+ affinity by touch hormones and elicitors, as well as readjustments of membrane potential, provides for effective adaptation to varying, prey-derived ammonium sources.

Experimental Procedures

Cloning of DmAMT1

Inspection of the available EST data from *Dionaea muscipula* [26] revealed the existence of an ammonium transporter homolog. PolyA-mRNA was isolated from 10 μg total RNA using Dynabeads (Invitrogen) according to the manufacturer's instructions. Using the SMARTer RACE kit (Takara Bio Europe/Clontech), a cDNA was generated from *Dionaea muscipula* whole-plant mRNA. The cDNA of DmAMT1 was amplified using gene-specific oligonucleotide primers directed toward the 5′ and 3′ region of DmAMT1 (GenBank accession number KC513764) and Advantage cDNA polymerase mix (Clontech), revealing a sequence identical to that expected from the EST data. The full-length clone was inserted into pJET1.2/blunt using the CloneJET PCR Cloning Kit (Fermentas). For heterologous expression in *Xenopus* oocytes, the generated cDNA of DmAMT1 was cloned into oocyte expression vectors (based on pGEM vectors) by an advanced uracil-excision-based cloning technique described by Nour-Eldin et al. [46]. Site-directed mutations were introduced with the QuikChange Site-Directed Mutagenesis Kit according to the manufacturer's instructions (Stratagene). For functional analysis, cRNA was prepared using the mMessage mMachine T7 Transcription Kit (Ambion). Oocyte preparation and cRNA injection have been described elsewhere [47]. For oocyte electrophysiological experiments, 10 ng DmAMT1 cRNA was injected.

Plant Material and Tissue Sampling

Dionaea muscipula plants were purchased from CRESCO Carnivora and grown in plastic pots at 22°C in a 16:8 hr light:dark photoperiod. The material for the expression analyses was harvested as follows: traps, petioles, and flowers were immediately frozen in liquid nitrogen. Additionally, secretory cells were isolated from the inner trap surface by gentle abrasion of the gland complexes with a razor blade. For induction of secretion, 100 μM coronatine solution (Sigma-Aldrich) was directly applied to the traps, and traps or glands were harvested after 24 hr.

Expression Analyses

RNA was separately isolated from each sample and transcribed into cDNA using M-MLV reverse transcriptase (Promega). Quantification of the actin transcript DmACT (GenBank accession number KC285589) and DmAMT1 transcripts were performed by real-time PCR as described elsewhere [48]. DmAMT1 transcripts were normalized to 10,000 molecules of DmACT. The following primers were used: DmAMT1LCfw, 5′-TTGCTACCAAGAAACAC-3′; DmAMT1LCrev, 5′-TGAGTTGATGTAAGGAG-3′; DmACTLCfw, 5′-TCTTTGATTGGGATGGAAGC-3′; and DmACTLCrev, 5′-GCAATGCCAGGGAACATAGT-3′.

Protein Digestion

To study the digestion products of insect prey, we produced insect powder from caterpillars of *Creatonotos transiens* (Lep.: Erebidae: Arctiinae) raised on artificial diet according to Bergomaz & Boppré [49]. In addition to the food, larvae were given access to glass fiber disks (Whatman GF/B25) impregnated with monocrotaline (Forstzoologisches Institut) as feeding stimulant. After 2 weeks of development, insects were dried, pulverized, and pooled to obtain homogenous insect powder used in the present study. Digestion was started by addition of 200 μl secretion fluid (pH 4.3), collected from *Dionaea muscipula*, to 5 mg, 10 mg, and 20 mg insect powder each. Samples were shaken for 15 hr at room temperature. Subsequently, samples were centrifuged, and 50 μl supernatant was used for amino acid analysis. In the same way, we analyzed digestion products of 5 mg, 10 mg, and 20 mg caseine (Sigma-Aldrich). Amino acids were extracted from supernatants with chloroform/methanol, as described elsewhere [50]. Freeze-dried extracts were resuspended in 1 ml of 0.02 M HCl prior to derivatization. For

derivatization, 5 μl resuspended extracts was mixed with 35 μl AccQ-Tag Ultra Borate buffer and 10 μl AccQ-Tag Reagent (Waters). For analysis of the compositions and concentrations of amino compounds, a Waters Acquity UPLC-System using an AccQ-Tag Ultra column (2.1 × 100 mm; Waters) was employed, as described by Luo et al. [50].

Ammonium Uptake

For study of NH_4^+ uptake by traps, 20 mg insect powder was dispensed in a solution containing 1 mM $^{15}NH_4^+$ (99 atom% 15N, Sigma-Aldrich), which was applied to traps. As a control, some plants were fed with a solution lacking $^{15}NH_4^+$. Uptake was stopped 3 hr after feeding. The traps were carefully and repeatedly rinsed and were then dried and pulverized. Between 1 and 2 mg dried material was weighed into tin capsules for elemental and isotope analysis. Samples were combusted in an elemental analyzer (NA 2500; CE Instruments) for C/N analysis, coupled to an Isotope Ratio Mass Spectrometer (Delta Plus/Delta Plus Plus XL; Finnigan MAT) by a Conflo II/III interface (Thermo-Finnigan). We used glutamate with known $^{15}N/^{14}N$ isotope ratio (Sigma-Aldrich) as laboratory standard.

Intracellular Measurements

Prior to measurements, the lobe of a cut trap was glued to a chamber bottom and left for recovery (30 min) in a standard solution containing 0.1 mM KCl, 10 mM $CaCl_2$, and 5 mM MES adjusted with Tris to pH 6. In the course of experiments, leaves were constantly perfused with the standard solution (1 ml/min).

For impalements, microelectrodes from borosilicate glass capillaries with filament (Hilgenberg,) were pulled on a horizontal laser puller (P2000, Sutter Instruments). They were filled with 300 mM KCl and connected via an Ag/AgCl half cell to a headstage (1 GΩ, HS-2A, Axon Instruments). A tip resistance was about 30 MΩ, while the input resistance of the headstage was 10^{13} Ω. The reference electrode was filled with 300 mM KCl as well. An IPA-2 amplifier (Applicable Electronics) was used. The cells were impaled by an electronic micromanipulator (NC-30, Kleindiek Nanotechnik).

Oocyte Recordings

In DEVC studies, oocytes were perfused with Tris/Mes-based buffers. The standard bath solution contained 10 mM Tris/Mes (pH 5.6), 1 mM $CaCl_2$, 1 mM $MgCl_2$, and 1 mM $LaCl_3$. The osmolality of each solution was adjusted to 220 mosmol/kg using D-sorbitol. To balance ionic strength for measurements with varying ammonium concentrations, we compensated with potassium to 10 mM. Solutions for selectivity measurements were composed of standard bath solution supplemented with 10 mM $NMDG^+$(N-methyl-d-glucamine), Li^+, Na^+, K^+, RB^+, Cs^+,$CH_3NH_3^+$, or NH_4^+ chloride salts. For temperature experiments, the bath solution passed through a heat exchanger in contact with Peltier elements on which the recording chamber was mounted. The temperature was measured with a small thermistor close to the oocyte. Data were analyzed using Igor Pro and Origin Pro 9.0G.

Accession Numbers

The GenBank accession number for DmAMT1 is KC513764.

Supplemental Information

Supplemental Information includes four figures and can be found with this article online at http://dx.doi.org/10.1016/j.cub.2013.07.028.

Acknowledgments

The research leading to these results has received funding from the European Research Council under the European Union's Seventh Framework Programme (FP/20010-2015)/ERC Grant Agreement number 250194-Carnivorom. Additionally, this work was supported by a grant from the Distinguished Scientist Fellowship Program, King Saud University (to R.H., E.N., and K.A.R.). We thank Brigitte Neumann for excellent technical assistance.

Received: February 18, 2013
Revised: May 7, 2013
Accepted: July 3, 2013
Published: August 15, 2013

References

1. Westhoff, C.M., Ferreri-Jacobia, M., Mak, D.O.D., and Foskett, J.K. (2002). Identification of the erythrocyte Rh blood group glycoprotein as a mammalian ammonium transporter. J. Biol. Chem. *277*, 12499–12502.
2. Weidinger, K., Neuhäuser, B., Gilch, S., Ludewig, U., Meyer, O., and Schmidt, I. (2007). Functional and physiological evidence for a rhesus-type ammonia transporter in *Nitrosomonas europaea*. FEMS Microbiol. Lett. *273*, 260–267.
3. Marini, A.M., Soussi-Boudekou, S., Vissers, S., and Andre, B. (1997). A family of ammonium transporters in *Saccharomyces cerevisiae*. Mol. Cell. Biol. *17*, 4282–4293.
4. Song, T., Gao, Q., Xu, Z., and Song, R. (2011). The cloning and characterization of two ammonium transporters in the salt-resistant green alga, *Dunaliella viridis*. Mol. Biol. Rep. *38*, 4797–4804.
5. Franco, A.R., Cárdenas, J., and Fernández, E. (1988). Two different carriers transport both ammonium and methylammonium in *Chlamydomonas reinhardtii*. J. Biol. Chem. *263*, 14039–14043.
6. Gessler, A., Schneider, S., Von Sengbusch, D., Weber, P., Hanemann, U., et al. (1998). Field and laboratory experiments on net uptake of nitrate and ammonium by the roots of spruce (*Picea abies*) and beech (*Fagus sylvatica*) trees. New Phytol. *138*, 275–285.
7. Couturier, J., Montanini, B., Martin, F., Brun, A., Blaudez, D., and Chalot, M. (2007). The expanded family of ammonium transporters in the perennial poplar plant. New Phytol. *174*, 137–150.
8. Sohlenkamp, C., Wood, C.C., Roeb, G.W., and Udvardi, M.K. (2002). Characterization of *Arabidopsis* AtAMT2, a high-affinity ammonium transporter of the plasma membrane. Plant Physiol. *130*, 1788–1796.
9. Søgaard, R., Alsterfjord, M., Macaulay, N., and Zeuthen, T. (2009). Ammonium ion transport by the AMT/Rh homolog TaAMT1;1 is stimulated by acidic pH. Pflugers Arch. *458*, 733–743.
10. Shelden, M.C., Dong, B., de Bruxelles, G.L., Trevaskis, B., Whelan, J., et al. (2001). *Arabidopsis* ammonium transporters, AtAMT1;1 and AtAMT1;2, have different biochemical properties and functional roles. Plant Soil *231*, 151–160.
11. Ortiz-Ramirez, C., Mora, S.I., Trejo, J., and Pantoja, O. (2011). PvAMT1;1, a highly selective ammonium transporter that functions as H+/NH4(+) symporter. J. Biol. Chem. *286*, 31113–31122.
12. D'Apuzzo, E., Rogato, A., Simon-Rosin, U., El Alaoui, H., Barbulova, A., Betti, M., Dimou, M., Katinakis, P., Marquez, A., Marini, A.M., et al. (2004). Characterization of three functional high-affinity ammonium transporters in *Lotus japonicus* with differential transcriptional regulation and spatial expression. Plant Physiol. *134*, 1763–1774.
13. Wood, C.C., Porée, F., Dreyer, I., Koehler, G.J., and Udvardi, M.K. (2006). Mechanisms of ammonium transport, accumulation, and retention in ooyctes and yeast cells expressing *Arabidopsis* AtAMT1;1. FEBS Lett. *580*, 3931–3936.
14. Boeckstaens, M., André, B., and Marini, A.M. (2008). Distinct transport mechanisms in yeast ammonium transport/sensor proteins of the Mep/Amt/Rh family and impact on filamentation. J. Biol. Chem. *283*, 21362–21370.
15. Gazzarrini, S., Lejay, L., Gojon, A., Ninnemann, O., Frommer, W.B., and von Wirén, N. (1999). Three functional transporters for constitutive, diurnally regulated, and starvation-induced uptake of ammonium into *Arabidopsis* roots. Plant Cell *11*, 937–948.
16. Ludewig, U., von Wirén, N., and Frommer, W.B. (2002). Uniport of NH4+ by the root hair plasma membrane ammonium transporter LeAMT1;1. J. Biol. Chem. *277*, 13548–13555.
17. Simon-Rosin, U., Wood, C., and Udvardi, M.K. (2003). Molecular and cellular characterisation of LjAMT2;1, an ammonium transporter from the model legume *Lotus japonicus*. Plant Mol. Biol. *51*, 99–108.
18. Loqué, D., and von Wirén, N. (2004). Regulatory levels for the transport of ammonium in plant roots. J. Exp. Bot. *55*, 1293–1305.
19. Ludewig, U., Wilken, S., Wu, B., Jost, W., Obrdlik, P., El Bakkoury, M., Marini, A.M., André, B., Hamacher, T., Boles, E., et al. (2003). Homo- and hetero-oligomerization of ammonium transporter-1 NH4 uniporters. J. Biol. Chem. *278*, 45603–45610.
20. Mayer, M., Dynowski, M., and Ludewig, U. (2006). Ammonium ion transport by the AMT/Rh homologue LeAMT1;1. Biochem. J. *396*, 431–437.
21. Rawat, S.R., Silim, S.N., Kronzucker, H.J., Siddiqi, M.Y., and Glass, A.D.M. (1999). *AtAMT1* gene expression and NH4+ uptake in roots of *Arabidopsis thaliana*: evidence for regulation by root glutamine levels. Plant J. *19*, 143–152.

22. Wang, M.Y., Glass, A.D.M., Shaff, J.E., and Kochian, L.V. (1994). Ammonium uptake by rice roots (III. Electrophysiology). Plant Physiol. *104*, 899–906.
23. Mayer, M., and Ludewig, U. (2006). Role of AMT1;1 in NH4+ acquisition in *Arabidopsis thaliana*. Plant Biol (Stuttg) *8*, 522–528.
24. Neuhäuser, B., Dynowski, M., Mayer, M., and Ludewig, U. (2007). Regulation of NH4+ transport by essential cross talk between AMT monomers through the carboxyl tails. Plant Physiol. *143*, 1651–1659.
25. Escalante-Pérez, M., Krol, E., Stange, A., Geiger, D., Al-Rasheid, K.A.S., Hause, B., Neher, E., and Hedrich, R. (2011). A special pair of phytohormones controls excitability, slow closure, and external stomach formation in the Venus flytrap. Proc. Natl. Acad. Sci. USA *108*, 15492–15497.
26. Schulze, W.X., Sanggaard, K.W., Kreuzer, I., Knudsen, A.D., Bemm, F., Thøgersen, I.B., Bräutigam, A., Thomsen, L.R., Schliesky, S., Dyrlund, T.F., et al. (2012). The protein composition of the digestive fluid from the venus flytrap sheds light on prey digestion mechanisms. Mol. Cell. Proteomics *11*, 1306–1319.
27. Darwin, C. (1875). Insectivorous Plants (New York: D Appleton & Co.).
28. Pantoja, O. (2012). High affinity ammonium transporters: molecular mechanism of action. Front Plant Sci *3*, 34.
29. Yan, J.B., Zhang, C., Gu, M., Bai, Z.Y., Zhang, W.G., Qi, T., Cheng, Z., Peng, W., Luo, H., Nan, F., et al. (2009). The *Arabidopsis* CORONATINE INSENSITIVE1 protein is a jasmonate receptor. Plant Cell *21*, 2220–2236.
30. Andrade, S.L., Dickmanns, A., Ficner, R., and Einsle, O. (2005). Crystal structure of the archaeal ammonium transporter Amt-1 from *Archaeoglobus fulgidus*. Proc. Natl. Acad. Sci. USA *102*, 14994–14999.
31. Khademi, S., O'Connell, J., 3rd, Remis, J., Robles-Colmenares, Y., Miercke, L.J., and Stroud, R.M. (2004). Mechanism of ammonia transport by Amt/MEP/Rh: structure of AmtB at 1.35 A. Science *305*, 1587–1594.
32. Loqué, D., Lalonde, S., Looger, L.L., von Wirén, N., and Frommer, W.B. (2007). A cytosolic trans-activation domain essential for ammonium uptake. Nature *446*, 195–198.
33. Lanquar, V., Loqué, D., Hörmann, F., Yuan, L., Bohner, A., Engelsberger, W.R., Lalonde, S., Schulze, W.X., von Wirén, N., and Frommer, W.B. (2009). Feedback inhibition of ammonium uptake by a phospho-dependent allosteric mechanism in *Arabidopsis*. Plant Cell *21*, 3610–3622.
34. Hille, B. (1992). Ionic Channels of Excitable Membranes, Second Edition (Sunderland: Sinauer Associates Inc.).
35. Woodhull, A.M. (1973). Ionic blockage of sodium channels in nerve. J. Gen. Physiol. *61*, 687–708.
36. Hedrich, R. (2012). Ion channels in plants. Physiol. Rev. *92*, 1777–1811.
37. Rea, P.A., Joel, D.M., and Juniper, B.E. (1983). Secretion and redistribution of chloride in the digestive glands of *Dionaea Muscipula* Ellis (Venus flytrap) upon secretion stimulation. New Phytol. *94*, 359–366.
38. Robins, R.J., and Juniper, B.E. (1980). The secretory cycle of *Dionaea Muscipula* Ellis. 1. The fine-structure and the effect of stimulation on the fine-structure of the digestive gland-cells. New Phytol. *86*, 279.
39. Rea, P.A. (1982). Fluid composition and factors that elicit secretion by the trap lobes of *Dionaea Muscipula* Ellis. Zeitschrift für Pflanzenphysiologie *108*, 255–272.
40. Joel, D.M., Rea, P.A., and Juniper, B.E. (1983). The cuticle of *Dionaea Muscipula* Ellis (Venus flytrap) in relation to stimulation, secretion and absorption. Protoplasma *114*, 44–51.
41. Rea, P.A. (1984). Evidence for the H+-co-transport of D-alanine by the digestive glands of *Dionaea Muscipula* Ellis. Plant Cell Environ. *7*, 363–366.
42. Becker, D., Stanke, R., Fendrik, I., Frommer, W.B., Vanderleyden, J., Kaiser, W.M., and Hedrich, R. (2002). Expression of the NH(+)(4)-transporter gene LEAMT1;2 is induced in tomato roots upon association with N(2)-fixing bacteria. Planta *215*, 424–429.
43. Schulze, W., Frommer, W.B., and Ward, J.M. (1999). Transporters for ammonium, amino acids and peptides are expressed in pitchers of the carnivorous plant *Nepenthes*. Plant J. *17*, 637–646.
44. Wyatt, G.R. (1961). The biochemistry of insect hemolymph. Annu. Rev. Entomol. *6*, 75–102.
45. Khan, K., and Elia, M. (1991). Factors affecting the stability of L-glutamine in solution. Clin. Nutr. *10*, 186–192.
46. Nour-Eldin, H.H., Hansen, B.G., Nørholm, M.H.H., Jensen, J.K., and Halkier, B.A. (2006). Advancing uracil-excision based cloning towards an ideal technique for cloning PCR fragments. Nucleic Acids Res. *34*, e122.
47. Becker, D., Dreyer, I., Hoth, S., Reid, J.D., Busch, H., Lehnen, M., Palme, K., and Hedrich, R. (1996). Changes in voltage activation, Cs+ sensitivity, and ion permeability in H5 mutants of the plant K+ channel KAT1. Proc. Natl. Acad. Sci. USA *93*, 8123–8128.
48. Escalante-Pérez, M., Jaborsky, M., Lautner, S., Fromm, J., Müller, T., Dittrich, M., Kunert, M., Boland, W., Hedrich, R., and Ache, P. (2012). Poplar extrafloral nectaries: two types, two strategies of indirect defenses against herbivores. Plant Physiol. *159*, 1176–1191.
49. Berrgomaz, R., and Boppré, M. (1986). A simple instant diet for rearing *Arctiidae* and other moths. Journal of The Lepidopterists' Society *40*, 131–137.
50. Luo, Z.B., Janz, D., Jiang, X., Göbel, C., Wildhagen, H., Tan, Y., Rennenberg, H., Feussner, I., and Polle, A. (2009). Upgrading root physiology for stress tolerance by ectomycorrhizas: insights from metabolite and transcriptional profiling into reprogramming for stress anticipation. Plant Physiol. *151*, 1902–1917.